

First-principles characterization of the structure and electronic structure of α -S and Rh-S chalcogenides

Oswaldo Diéguez

Institut de Ciència de Materials de Barcelona (ICMAB-CSIC), Campus UAB, 08193 Bellaterra, Spain

Nicola Marzari

Department of Materials Science and Engineering, Massachusetts Institute of Technology, 77 Massachusetts Avenue, Cambridge, Massachusetts 02139, USA

(Received 12 August 2009; revised manuscript received 25 November 2009; published 22 December 2009)

We have used first-principles calculations to study the structural, electronic, and thermodynamic properties of the three known forms of Rh-S chalcogenides: Rh_2S_3 , Rh_3S_4 , and $\text{Rh}_{17}\text{S}_{15}$. Only the first of these materials of interest for catalysis had been studied previously within this approach. We find that $\text{Rh}_{17}\text{S}_{15}$ crystallizes in a $Pm\bar{3}m$ centrosymmetric structure, as believed experimentally but never confirmed. We show band structures and densities of states for these compounds. Finally, we also investigated the ground-state structure of solid sulfur (α -S), one of the few elements that represents a challenge for full first-principles calculations due to its demanding 128-atom unit cell and dispersion interactions between S_8 units.

DOI: [10.1103/PhysRevB.80.214115](https://doi.org/10.1103/PhysRevB.80.214115)

PACS number(s): 61.50.-f, 71.20.-b

I. INTRODUCTION

There is currently a growing interest in rhodium sulfide materials because of the potential of transition-metal chalcogenides as catalysts in fuel cells, substituting expensive and scarce platinum.^{1,2} Rhodium sulfide possesses promising characteristics, from significant activity in acid electrolytes to selectivity toward oxygen reduction reaction in large concentrations of methanol.³ Recently, a commercially available carbon-supported Rh_xS_y electrocatalyst has shown a superior stability and performance over a sample of other chalcogenides while being free of the toxicity problems intrinsic to those containing selenium.⁴ Other than in fuel cells, rhodium sulfide is useful as a catalyst in situations such as efficient electrolysis of aqueous HCl solutions for the industrial recovery of high-value chlorine gas.⁵

The Rh_xS_y material used for electrocatalysis contains a mixture of the three phases of rhodium sulfide that are positively known to exist: Rh_2S_3 , Rh_3S_4 , and $\text{Rh}_{17}\text{S}_{15}$. Despite the interest on their catalytic properties, not much is known about these materials, in part due to their complex crystal structures (with 20, 42, and 64 atoms per unit cell, respectively). In this situation, we have used first-principles calculations as an effective tool to extract valuable information about these systems. In the same spirit, and as a way to validate our methodology, we also investigated the structural properties of the ground state of pure sulfur (α -S). Sulfur is one of the very few elements for which full first-principles relaxation calculations have not been performed (boron being another element known for the difficulties that its crystalline ground state presents⁶).

The rest of this paper is organized as follows. We describe the method we used in Sec. II, present our main results in Sec. III, and summarize our work in Sec. IV.

II. METHODOLOGY

For our calculations, we have used density-functional theory (DFT) (Ref. 7) in the Kohn-Sham framework,⁸ as

implemented in the PWSCF program of the QUANTUM-ESPRESSO package.⁹ For the exchange-correlation functional we employed the generalized-gradient approximation (GGA) functional developed by Perdew, Burke, and Ernzerhof (PBE) (Ref. 10) since it is known that GGA gives somewhat better results than the simpler local-density approximation when describing the structural properties of this kind of transition-metal sulfides.¹¹ The electron-ion interactions are described through the use of ultrasoft pseudopotentials.¹² These pseudopotentials were generated with scalar-relativistic calculations in the $4d^75s^2$ configuration for Rh and in the $3s^23p^4$ configuration for S. More specific details about the pseudopotentials can be found in Ref. 13.

The Kohn-Sham equations⁸ were solved self-consistently by using a plane-wave basis set and the integrations in reciprocal space were performed using Monkhorst-Pack grids.¹⁴ The amount of plane waves and grid points used depended on the system studied and more details are given in the next section.

III. RESULTS

As a way to control the numerical approximation involved in our methodology, we studied the properties of the isolated crystalline elements Rh and S, and we compared the results with the well-known experimental ones. In the process we have done what we believe are the first DFT calculations with full relaxation of the 128-atom unit cell of the most stable phase of S at ambient conditions. Then we then applied the same methodology to compute the structural and electronic properties of three Rh-S compounds: Rh_2S_3 , Rh_3S_4 , and $\text{Rh}_{17}\text{S}_{15}$.

A. Pure elements

1. Rhodium

Rhodium is a precious metal that crystallizes in a face-centered-cubic lattice with one atom per unit cell, corre-

sponding to space group 225 ($Fm\bar{3}m$). Our DFT calculations for crystalline Rh use a plane-wave cutoff of 30 Ry and a $4 \times 4 \times 4$ k -point mesh. We obtained a optimized lattice parameter of 3.862 Å (Rh-Rh distance of 2.731 Å) and a bulk modulus of 258 GPa. This shows a good agreement with experimental values (3.80 Å and 270 GPa, respectively) and with other theoretical calculations (see Ref. 15, and references therein).

2. Sulfur

Sulfur can crystallize in around 30 different phases depending on pressure and temperature, a number that makes it the chemical element with the highest number of allotropes in the periodic table.¹⁶ At ambient pressure it forms structures with a very small packing factor. 20 of those are composed of molecular rings with 6–20 sulfur atoms each. There also exist polymeric structures formed by molecular chains. As pressure increases the structures get more closely packed and in the megabar regime sulfur becomes a metal with a superconducting temperature of 17 K.¹⁷

At ambient conditions the most stable phase of sulfur is α -S in which S_8 molecules crystallize in the orthorhombic space group 70 ($Fddd$). Figure 1(a) shows the unit cell of α -S, containing 16 S_8 molecules. Due to the interactions with its neighbors, the original D_{4d} symmetry of each S_8 molecule is lost and instead it has C_2 symmetry with the rotation axis along the c axis of the solid, as shown in Fig. 1(b).

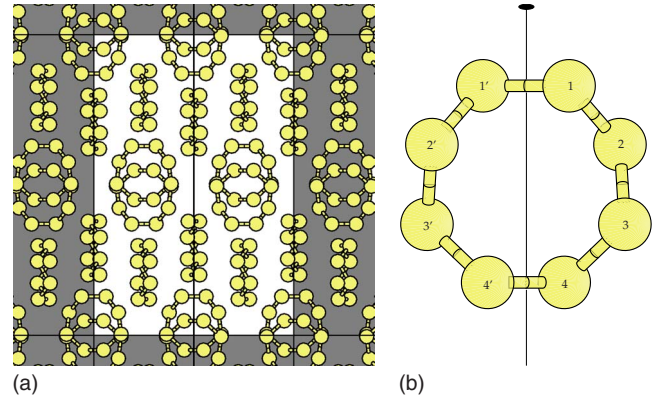


FIG. 1. (Color online) (a) Structure of α -S viewed from the $[110]$ axis, with the $[001]$ axis along the length of the page; the unit cell (white background) contains 16 S_8 molecules. (b) One of the S_8 molecules, showing the C_2 axis along the $[001]$ direction of the crystal; the labels on the atoms will be used in the text to identify them.

We have performed DFT calculations for α -S using a plane-wave cutoff of 30 Ry and the Γ point for the reciprocal space integrals. The plane-wave cutoff was high enough as to provide results that were converged better than one part in 1000 for the bond length, bond angles, and dihedral angles of the S_8 molecule. We tested convergence with respect to k -point sampling by doing a calculation at fixed experimental

TABLE I. Lattice parameters, bond lengths, bond angles, and dihedral angles for α -S as obtained experimentally (Ref. 18) and computed in this work. The three theory columns refer to a fully relaxed cell, to a cell with fixed experimental lattice vectors, and to the relaxation of the isolated S_8 molecule.

	Experiment	Theory (this work)		
	α -S	α -S	α -S (fixed cell)	Isolated S_8
a	10.4646 Å	12.772 Å	(10.4646 Å)	
b	12.8660 Å	14.639 Å	(12.8660 Å)	
c	24.4860 Å	26.045 Å	(24.4860 Å)	
S(1)-S(1')	2.055 Å	2.070 Å	2.059 Å	2.070 Å
S(1)-S(2)	2.054 Å	2.071 Å	2.067 Å	2.070 Å
S(2)-S(3)	2.057 Å	2.070 Å	2.066 Å	2.070 Å
S(3)-S(4)	2.056 Å	2.072 Å	2.069 Å	2.070 Å
S(4)-S(4')	2.050 Å	2.068 Å	2.061 Å	2.070 Å
Mean S-S	2.055 Å	2.070 Å	2.066 Å	2.070 Å
S(1')-S(1)-S(2)	109.02°	109.4°	110.3°	109.3°
S(1)-S(2)-S(3)	108.01°	109.5°	109.0°	109.3°
S(2)-S(3)-S(4)	107.39°	109.1°	108.5°	109.3°
S(3)-S(4)-S(4')	108.42°	109.2°	109.0°	109.3°
Mean S-S-S	108.2°	109.3°	109.2°	109.3°
S(2')-S(1')-S(1)-S(2)	95.26°	96.8°	94.5°	97.2°
S(1')-S(1)-S(2)-S(3)	98.12°	97.1°	96.4°	97.2°
S(1)-S(2)-S(3)-S(4)	100.81°	97.1°	98.8°	97.2°
S(2)-S(3)-S(4)-S(4')	98.84°	97.2°	98.2°	97.2°
S(3)-S(4)-S(4')-S(3')	96.94°	97.6°	96.9°	97.2°
Mean S-S-S-S	98.5°	97.2°	97.3°	97.2°

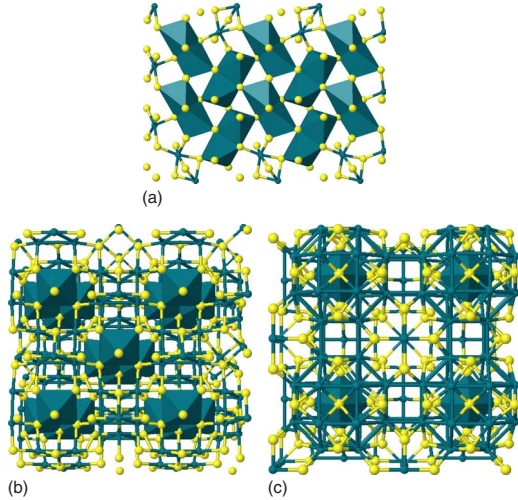


FIG. 2. (Color online) Atomic structures obtained in this work for Rh-S materials: (a) $3 \times 2 \times 3$ supercell for orthorhombic Rh_2S_3 , showing one of the two layers of face-sharing RhS_6 octahedra present in the primitive 20-atom unit cell; (b) $2 \times 2 \times 2$ supercell for monoclinic Rh_3S_4 , showing the octahedra surrounding two of the four inequivalent Rh atoms and the bonds between the other two types of Rh atoms; (c) $2 \times 2 \times 1$ supercell for cubic $\text{Rh}_{17}\text{S}_{15}$, showing the octahedra surrounding one of the four inequivalent Rh atoms.

lattice parameters using four grid points, including the Γ point and three more points at the boundary of the Brillouin zone. After optimization the geometrical features of the atomic arrangement did not show any important change, with the bond lengths varying less than 0.4% and the angles varying less than 0.8%. Table I shows the structural results we have obtained once the atoms were relaxed (using both in the fixed experimental cell vectors and free cell vectors) and a comparison with experimental data. The lengths of the cell vectors are larger than the experimental results by 22.0%, 13.8%, and 6.4%. However, the S-S bonds in every S_8 ring are better than 1% in agreement with experiments. Moreover, these rings show very similar geometrical features when the cell used is the smaller experimental one or when the computations are performed on an isolated ring. These facts are one more illustration of the inability of functionals such as PBE to deal with nonlocal van der Waals interactions like the ones between S_8 rings in orthorhombic sulfur. Very promising developments within DFT to deal with systems where these interactions are important exist¹⁹ and they have been made computationally effective very recently.²⁰

B. Rh-S compounds

The rhodium sulfide compounds seem to have been investigated first by Juza *et al.*,²¹ who found several phases for these chalcogenides in 1935. One of them, believed to be “ Rh_9S_8 ,” turned out to be a superconductor with a transition temperature of 5.8 K.²² Almost 30 years later, Geller showed that its composition was actually $\text{Rh}_{17}\text{S}_{15}$ and that this is a cubic material belonging to one of three possible space groups: $Pm\bar{3}m(221, O_h)$, $P\bar{4}3m(215, T_d)$, or $P432(207, O)$.²³

TABLE II. Lattice parameters, Wickoff atomic positions, and nearest-neighbor distances in Rh_2S_3 (space group 60, $Pbcn$). The experimental data are from Ref. 24.

		Experiment	Theory (this work)
	a	8.462 Å	8.577 Å
	b	5.985 Å	6.049 Å
	c	6.138 Å	6.211 Å
Rh(1)	$8d$	0.10645	0.1071
		0.2517	0.2513
S(1)	$8d$	0.0338	0.0331
		0.1518	0.1512
S(2)		0.3906	0.3895
		0.3930	0.3941
	$4c$	0	0
		0.9525	0.9528
		1/4	1/4

It was not possible at the time to make a choice of the most probable of the three space groups to which the crystal might belong. No further attempts seem to have been made in order to pursue this question. Most of the literature published afterward refers to $\text{Rh}_{17}\text{S}_{15}$ as the centrosymmetric structure $Pm\bar{3}m$ since that is the one for which lowest standard errors were obtained in the crystallographic analysis, even if Geller himself writes that “this in itself does not necessarily mean that it is the most probable one.”²³ A mineral with composition $\text{Rh}_{17}\text{S}_{15}$ receives the name of prassoite or miassite.

Shortly after $\text{Rh}_{17}\text{S}_{15}$ was characterized, the structure of Rh_2S_3 was also determined.²⁴ This is a diamagnetic semiconductor with orthorhombic space group $Pbcn(60, D_{2h})$. The authors also pointed out the impossibility of preparing a hypothetical “ RhS_2 ” phase that had been reported previously, stating that attempts to do so led to a two-phase mixture containing elementary S and Rh_2S_3 . Rh_2S_3 is found as a mineral called bowieite, where part of the Rh atoms are substituted by Pt and Ir.

The original work by Juza *et al.*²¹ described also a rhodium sulfide of the form Rh_3S_4 . However, it was not until 2000 that the characterization of this structure was published,²⁵ after Rh_3S_4 was synthesized at high temperature. This is a monoclinic structure with space group $C2/m(12, C_{2h})$. It corresponds to a metal that shows a weak paramagnetism down to 4.5 K.²⁵ Recently, the mineral kingstonite of ideal composition Rh_3S_4 has been found by the Bir river in Ethiopia, although again with Ir and Pt substituting to some degree Rh atoms.²⁶

In the following we apply a first-principles method to investigate the three materials described (Rh_2S_3 , Rh_3S_4 , and $\text{Rh}_{17}\text{S}_{15}$). These are, as far as we know, all the rhodium sulfides that have been characterized experimentally. Only Rh_2S_3 had been previously studied from first principles.¹¹

I. Structures

We relaxed the unit-cell vectors and atomic positions of the three materials studied. After careful tests, we used a

TABLE III. Lattice parameters, Wickoff atomic positions, and nearest-neighbor distances for Rh_3S_4 (space group 12, $C2/m$). The experimental data are from Ref. 25.

		Experiment	Theory (this work)
	a	10.29 Å	10.491 Å
	b	10.67 Å	10.899 Å
	c	6.212 Å	6.326 Å
	β	107.7°	107.9°
Rh(1)	8j	0.36278	0.3616
		0.14491	0.1464
		0.4501	0.4499
Rh(2)	4i	0.3509	0.3495
		0	0
		0.0546	0.0550
Rh(3)	2c	0	0
		0	0
		1/2	1/2
Rh(4)	4g	0	0
		0.1596	0.1611
		0	0
S(1)	4i	0.4165	0.4157
		0	0
		0.7291	0.7256
S(2)	8j	0.1262	0.1260
		0.1582	0.1586
		0.3854	0.3853
S(3)	4i	0.1182	0.1171
		0	0
		0.8883	0.8883
S(4)	8j	0.3493	0.3501
		0.2111	0.2089
		0.0990	0.1004

plane-wave cutoff of 40 Ry and Monkhorst-Pack grids of $2 \times 2 \times 2$. This implied using eight nonequivalent k points for Rh_2S_3 and Rh_3S_4 , and four nonequivalent k points for $\text{Rh}_{17}\text{S}_{15}$.

Figure 2(a) shows the atomic arrangement we obtained for orthorhombic Rh_3S_4 . The structural information for this material is summarized in Table II. In this crystal there is only one inequivalent Rh atom that is surrounded by six S atoms located at the vertices of a distorted octahedron. There are two inequivalent S atoms, both surrounded by four Rh atoms forming a distorted tetrahedron. The whole structure can be described as an alternating stacking sequence of octahedron pair layers along [010], where each layer is related to a neighboring one by a b -glide reflection. The cell parameters computed agree very well with experiment, the errors being 1.4% (a), 1.1% (b), and 1.2% (c). Apart from slightly larger bonds, the PBE approximation gives excellent geometric predictions for this compound, finding exactly the same patterns of distortion that are found experimentally. The closest Rh-Rh distance is 3.208 Å, substantially larger than the Rh-Rh bond in pure Rh (2.731 Å). Our findings are very

TABLE IV. Lattice parameters, Wickoff atomic positions, and nearest-neighbor distances for $\text{Rh}_{17}\text{S}_{15}$ (space group 221, $Pm\bar{3}m$). The experimental data are from Ref. 23.

		Experiment	Theory (this work)
	a	9.911 Å	10.025 Å
Rh(1)	24m	0.3564	0.3574
		0.3564	0.3574
		0.1435	0.1426
Rh(2)	6e	0	0
		0	0
		0.2338	0.2373
Rh(3)	3d	0	0
		0	0
		1/2	1/2
Rh(4)	1b	1/2	1/2
		1/2	1/2
		1/2	1/2
S(1)	12j	0.1696	0.1696
		0.1696	0.1696
		1/2	1/2
S(2)	12i	0.2310	0.2293
		0.2310	0.2293
		0	0
S(3)	6f	1/2	1/2
		1/2	1/2
		0.2643	0.2630

close to those of Raybaud *et al.*,¹¹ who used a similar methodology.

Rh_3S_4 has a complex monoclinic unit cell with 42 atoms, of which four Rh and four S are inequivalent. This structure is shown in Fig. 2(b) and its geometrical properties are listed in Table III together with experimental values. Two of the Rh atoms are still six coordinated with S atoms forming a distorted octahedron. However, the other two inequivalent Rh atoms form Rh_6 clusters surrounded by S atoms. In these clusters, the Rh-Rh bond lengths are similar to the ones in pure Rh. Again, our DFT results show good agreement for lattice parameters (with errors of 1.9%, 2.1%, and 1.8%, for a , b , and c) and reproduce very well all the features of the atomic distribution in the material.

As mentioned in the beginning of this section, the crystallographic analysis was unable to conclude whether $\text{Rh}_{17}\text{S}_{15}$ belongs to group $Pm\bar{3}m(221, O_h)$, $P\bar{4}3m(215, T_d)$, or $P432(207, O)$.²³ We have performed first-principles calculations starting from each of these 64-atom unit-cell structures, including also atoms randomly displaced from them to do a more thorough exploration of the energy surface. In all cases the final relaxed state corresponds to the cubic $Pm\bar{3}m$ case. Since this point group contains the symmetry operations of both $P\bar{4}3m$ and $P432$ we conclude that this is indeed the ground state of $\text{Rh}_{17}\text{S}_{15}$ and that the other two structures are not stable. The structure and crystallographic data obtained are contained in Fig. 2(c) and Table IV. The four

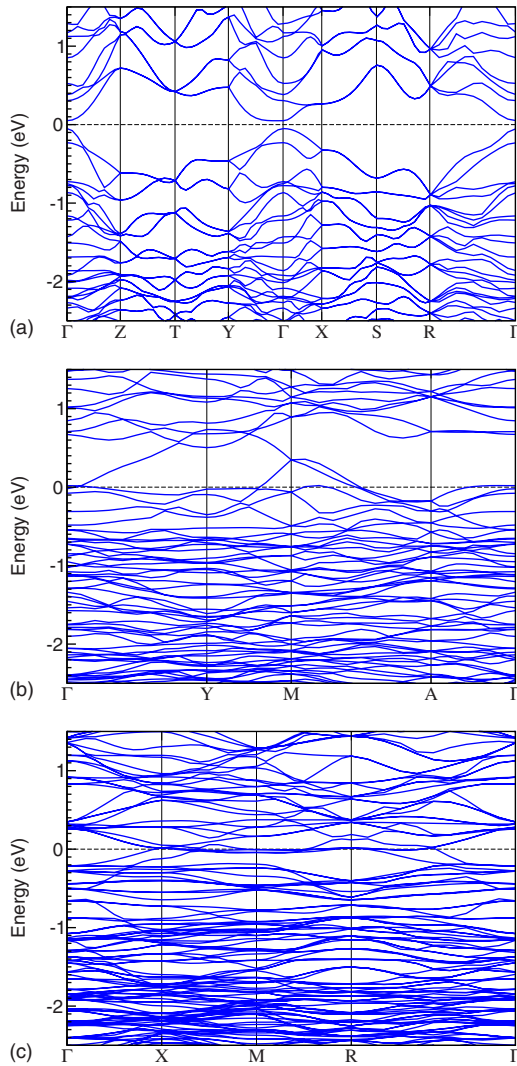


FIG. 3. (Color online) Band structure for (a) Rh_2S_3 , (b) Rh_3S_4 , and (c) $\text{Rh}_{17}\text{S}_{15}$.

inequivalent Rh atoms have different environments; the central one at $(1/2, 1/2, 1/2)$ is surrounded by six S atoms forming a perfect octahedron while the other three Rh atoms have four S neighbors each. The Rh-Rh bonds get stronger than in the previous two materials, being around 3.5% shorter than in the case of pure Rh. Our DFT calculations reproduce all the experimental structural details, showing a lattice parameter and bond lengths around 1% larger.

2. Electronic properties

The band structures and densities of states computed using first-principles calculations can be seen in Figs. 3 and 4. As the Rh content increases, the materials go from narrow-gap insulator (Rh_2S_3) to metals (Rh_3S_4 and $\text{Rh}_{17}\text{S}_{15}$).

The band gap we obtained for Rh_2S_3 is 0.10 eV, in excellent agreement with the results of Raybaud *et al.*,²⁷ who obtained a gap of 0.09 eV. Our density of states is also very similar to theirs; the $4d$ electrons of Rh are split in the t_{2g} and e_g manifolds by the octahedral field, with the Fermi level laying in between.

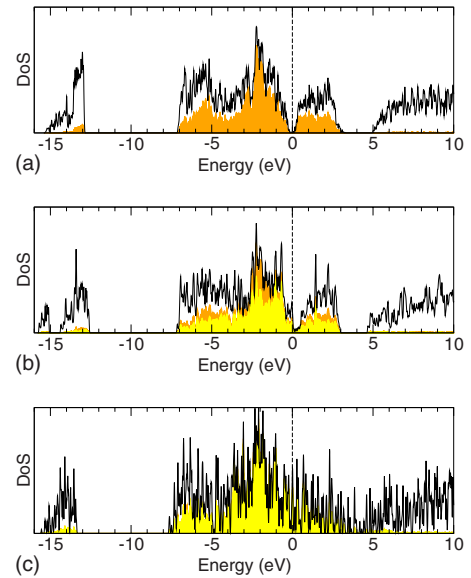


FIG. 4. (Color online) Density of states for (a) Rh_2S_3 , (b) Rh_3S_4 , and (c) $\text{Rh}_{17}\text{S}_{15}$. Black lines represent the total density of states and dark (light) shadow areas represent the density of states projected on the d orbitals of the Rh atoms (the Rh atoms bonded to other Rh atoms).

The higher concentration of Rh in Rh_3S_4 pushes some of the Rh atoms to form bonds of similar length to the ones in the pure metal. This causes the gap to close, being populated mainly by the d states of the Rh clusters. Our results show that the electronic analysis made by Beck and Hilbert²⁵ using extended Hückel calculations is quantitatively correct.

In the case of $\text{Rh}_{17}\text{S}_{15}$, only one of the four inequivalent atoms is surrounded by S atoms forming a (regular) octahedron. There are strong bonds between the rest of Rh atoms, and the band structure and density of states for this material shows its clear metallic character.

3. Formation enthalpy

We have computed the cohesive energy of the three Rh-S materials by comparing their energies in the ground state with the energy of the isolated atoms of Rh and S. Our results are 4.73 eV/atom (Rh_2S_3), 4.83 eV/atom (Rh_3S_4), and 5.05 eV/atom ($\text{Rh}_{17}\text{S}_{15}$). The first of these is in good agreement with the experimental (4.61 eV/atom) and theoretical (4.84 eV/atom) values reported in Ref. 11.

A useful reference for alloys is their enthalpy of formation, computed as the difference between their cohesive energy and the (weighted) one of the pure elements that form them. Figure 5 contains the formation enthalpy for each of the rhodium sulfides, using α -S and fcc Rh as the end components. It shows a convex hull, as expected since the three materials are stable. In fact, as mentioned in the introduction, the Rh-S electrocatalyst commercially available contains a mixture of the three.⁴

IV. SUMMARY

In this paper we present a first-principles study of the three rhodium sulfides that are positively known to exist. We

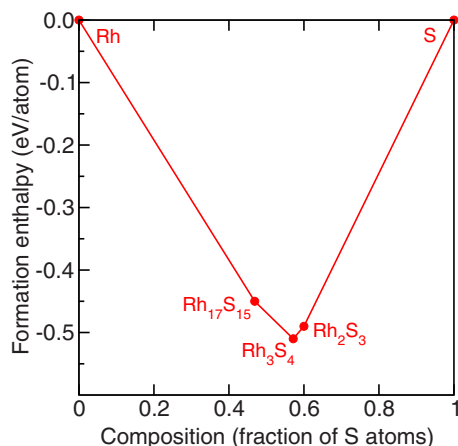


FIG. 5. (Color online) Formation enthalpy for Rh-S materials.

have obtained the relaxed structures for these materials of interest for catalysis. For Rh_2S_3 and Rh_3S_4 the crystallographic structures we find are very similar to the ones found experimentally while for $\text{Rh}_{17}\text{S}_{15}$ we identify one of the three configurations proposed experimentally as the one the atoms

take. We have computed the band structure and density of states for the three compounds, something that had only been done before for Rh_2S_3 using first principles. We also present an analysis of the energetics of these chalcogenides, showing the convex hull graph for these alloys. As part of this study, we also performed what we believe is the first full optimization of the 128-atom unit cell of α -S using DFT, showing how the PBE approximation gets correctly the S-S bonds in the compound but that it is necessary to include a further correction to take into account the van der Waals interactions between S_8 rings in the structure.

ACKNOWLEDGMENTS

We thank J. M. Ziegelbauer and S. Mukerjee for valuable discussions, E. Canadell for a critical reading of the manuscript, and N. Singh-Miller for computational assistance. We have used the XCRYSDEN (Ref. 28) and JMOL (Ref. 29) graphics programs, and the Bilbao Crystallographic Server (Ref. 30). We acknowledge support from the MURI under Grant No. DAAD 19-03-1-0169. O.D. acknowledges support from the *Ramón y Cajal* program of the Spanish Government.

- ¹N. A. Vante and H. Tributsch, *Nature (London)* **323**, 431 (1986).
- ²N. A. Vante, W. Jaegermann, H. Tributsch, W. Hönle, and K. Yvon, *J. Am. Chem. Soc.* **109**, 3251 (1987).
- ³J. M. Ziegelbauer, D. Gatewood, A. F. Gullá, D. E. Ramaker, and S. Mukerjee, *Electrochem. Solid-State Lett.* **9**, A430 (2006).
- ⁴J. M. Ziegelbauer, V. S. Murthi, C. O'Laoire, A. F. Gullá, and S. Mukerjee, *Electrochim. Acta* **53**, 5587 (2008).
- ⁵A. F. Gullá, L. Gancs, R. J. Allen, and S. Mukerjee, *Appl. Catal., A* **326**, 227 (2007).
- ⁶T. Ogitsu, F. Gygi, J. Reed, Y. Motome, E. Schwegler, and G. Galli, *J. Am. Chem. Soc.* **131**, 1903 (2009).
- ⁷P. Hohenberg and W. Kohn, *Phys. Rev.* **136**, B864 (1964).
- ⁸W. Kohn and L. J. Sham, *Phys. Rev.* **140**, A1133 (1965).
- ⁹P. Giannozzi, S. Baroni, N. Bonini, M. Calandra, R. Car, C. Cavazzoni, D. Ceresoli, G. Chiarotti, M. Cococcioni, I. Dabo, A. Dal Corso, S. Fabris, G. Fratesi, S. de Gironcoli, R. Gebauer, U. Gerstmann, C. Gougoussis, A. Kokalj, M. Lazzeri, L. Martin-Samos, N. Marzari, F. Mauri, R. Mazzarello, S. Paolini, A. Pasquarello, L. Paulatto, C. Sbraccia, S. Scandolo, G. Sclauzero, A. Seitsonen, A. Smogunov, P. Umari, and R. Wentzcovitch, *J. Phys.: Condens. Matter* **21**, 395502 (2009).
- ¹⁰J. P. Perdew, K. Burke, and M. Ernzerhof, *Phys. Rev. Lett.* **77**, 3865 (1996).
- ¹¹P. Raybaud, G. Kresse, J. Hafner, and H. Toulhoat, *J. Phys.: Condens. Matter* **9**, 11085 (1997).
- ¹²D. Vanderbilt, *Phys. Rev. B* **41**, 7892 (1990).
- ¹³See files Rh.pbe-nd-rrkjus.UPF and S.pbe-van_bm.UPF at <http://www.pwscf.org/pseudo.php>
- ¹⁴H. J. Monkhorst and J. D. Pack, *Phys. Rev. B* **13**, 5188 (1976).
- ¹⁵M. Pozzo, G. Carlini, R. Rosei, and D. Alfè, *J. Chem. Phys.* **126**, 164706 (2007).
- ¹⁶R. Steudel and B. Eckert, *Top. Curr. Chem.* **230**, 1 (2003).
- ¹⁷V. V. Struzhkin, R. J. Hemley, H.-K. Mao, and Y. A. Timofeev, *Nature (London)* **390**, 382 (1997).
- ¹⁸S. J. Rettig and J. Trotter, *Acta Crystallogr., Sect. C: Cryst. Struct. Commun.* **C43**, 2260 (1987).
- ¹⁹M. Dion, H. Rydberg, E. Schröder, D. C. Langreth, and B. I. Lundqvist, *Phys. Rev. Lett.* **92**, 246401 (2004).
- ²⁰G. Román-Pérez and J. M. Soler, *Phys. Rev. Lett.* **103**, 096102 (2009).
- ²¹R. Juza, O. Hülsmann, K. Meisel, and W. Biltz, *Z. Anorg. Chem.* **225**, 369 (1935).
- ²²B. T. Matthias, E. Corenzwit, and C. E. Miller, *Phys. Rev.* **93**, 1415 (1954).
- ²³S. Geller, *Acta Crystallogr.* **15**, 1198 (1962).
- ²⁴E. Parthé, E. Hohnke, and F. Hulliger, *Acta Crystallogr.* **23**, 832 (1967).
- ²⁵J. Beck, and T. Hilbert, *Z. Anorg. Chem.* **626**, 72 (2000).
- ²⁶C. J. Stanley, A. J. Criddle, J. Spratt, A. C. Roberts, J. T. Szymański, and M. D. Welch, *Miner. Mag.* **69**, 447 (2005).
- ²⁷P. Raybaud, J. Hafner, G. Kresse, and H. Toulhoat, *J. Phys.: Condens. Matter* **9**, 11107 (1997).
- ²⁸A. Kokalj, *Comput. Mater. Sci.* **28**, 155 (2003). Code available at <http://www.xcrysden.org/>.
- ²⁹JMOL is an open-source Java viewer for chemical structures in three dimensions available at <http://www.jmol.org/>
- ³⁰I. Aroyo, J. M. Perez-Mato, C. Capillas, E. Kroumova, S. Ivantchev, G. Madariaga, A. Kirov, and H. Wondratschek, *Z. Kristallogr.* **221**, 15 (2006); M. I. Aroyo, A. Kirov, C. Capillas, J. M. Perez-Mato, and H. Wondratschek, *Acta Crystallogr., Sect. A: Found. Crystallogr.* **A62**, 115 (2006).